REMOTE SENSING AND CHARACTERIZATION OF ANOMALOUS DEBRIS

R. Sridharan, W. Beavers, R. Lambour, E.M. Gaposchkin, J. Kansky,

Lincoln Laboratory, Massachusetts Institute of Technology,
244 Wood Street, Lexington, MA 02173

E. Stansbery

NASA/Johnson Space Center
2400 NASA Rd. 1, Mail Code SN3, Houston, TX 77058

ABSTRACT

Analysis of orbital debris data has shown a band of anomalously high debris concentration between 800 Km. and 1000 Km. Detective work by NASA has shown the likely origin to be leaking coolant fluid from nuclear power sources that powered a now defunct Soviet space-based series of ocean surveillance satellites.

A project has been in progress at MIT Lincoln Laboratory to detect, track and characterize a small sample of the anomalous debris. The primary sensors used for the purpose are the Haystack radar, the Millstone hill radar, TRADEX and the Firepond optical observatory. The major questions being addressed are:

1. What are the size and shape of the sample set?
2. Can we infer the composition of the material the droplets are made of?

The techniques being used to detect, track and characterize the sample set will be described in this paper. Results of the characterization analysis will also be presented.

1. INTRODUCTION

Remote sensing of small debris in space is a challenging task because of the low signal-to-noise (S/N) ratios that can be attained by ground-based sensors for detection and tracking . However, characterization of space debris is important as it is one of the factors affecting the short-term and long-term safety of humans in space and also of orbiting spacecraft. We present in this report techniques developed at MIT Lincoln Laboratory for remote sensing and characterization of a particular debris field and discuss the results. High power radars and high sensitivity optical systems were used for this effort because of their unique and complementary capabilities.

1.1. Debris and the Haystack Radar

NASA/JSC has been engaged in an extensive study of debris in space for over a decade. The study was triggered by the potential of significant damage to the space station and the shuttle due to impact of debris. The typical velocity of impact would be ~10 Km/s and hence even small centimeter-sized debris can cause catastrophic damage. NASA/JSC developed a model to represent the density distribution of debris in space. This model has been revised and corrected using data from actual impacts on the shuttle, the LDEF and, for the most significant threat sizes of ~5 mm. to 5cm., from the Haystack radar (Refs.1-2).

Figure 1 gives the pertinent characteristics of the Haystack radar. The radar is operated in a "stare" mode for debris data collection, *ie.,* the radar is pointed at an azimuth and elevation over a slant range extent. The earth's rotation creates a scan of space. Data are recorded whenever a preset threshold of detection S/N ratio is exceeded.

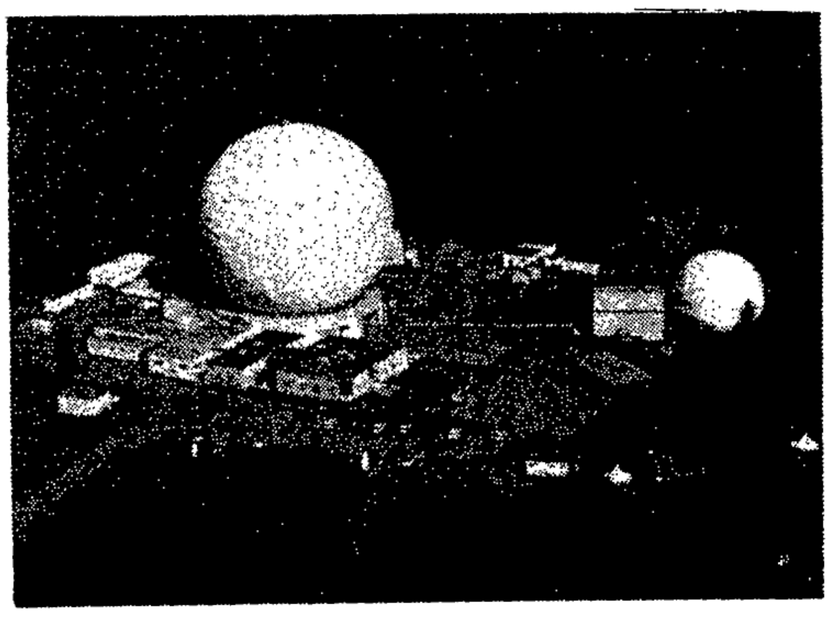

Fig. 1. Haystack Radar
(10 Ghz x-band radar, 36 M. antenna, 1FOV 1 mrad, S/N ratio of 58 dB on a 1 sq. m. target at a range of 1000 km.)

These data are processed by NASA/JSC and result in cumulative statistics of detection as well

as orbit and size characterization. One method of presenting the results is shown in Fig. 2 which is taken from Ref. 2. This figure represents the rate of detections in the Haystack beam when pointed at zenith as a function of the altitude of detection. The lower curve is a simulation of the rate for the known catalog carried by US Air Force's Space Command while the upper curve is the rate of detections processed from the Haystack data. NASA/JSC estimates that the total rate across all altitudes sampled (< 1500 Km.) is ~6.25 objects/hour.

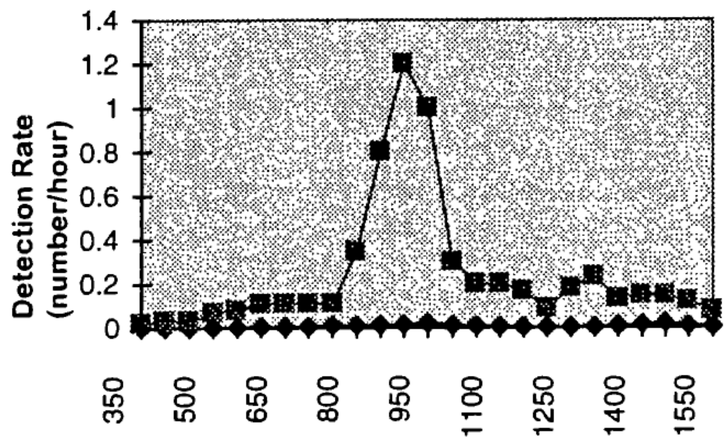

Fig. 2: Debris Detection Rate from Haystack Radar

1.2. Anomalous Debris

Most of the debris detections shown in Fig. 2 are concentrated in the altitude range between 800 Km. and 1000 Km. though there is a noticeable but smaller peak in rate of detection at ~1400 Km. The subject of this report are the debris in the 800 to 1000 Km. region. NASA/JSC has analyzed these detections extensively and concluded that (Ref. 3):

1. the debris are primarily small (< 2 cm. size) and largely spherical in shape;
2. the debris are concentrated in orbits of inclination 65^0 and altitudes of 900 - 1000 Km.;
3. the debris are primarily in circular orbits;
4. the debris are likely to be leaked Na-K coolant from the Bouk class of nuclear power sources of a Soviet satellite system, called RORSAT (Ref. 4) which were put into this type of orbit for long-term storage to allow the radio-activity to decay;
5. there are 50000-70000 such debris > 8 mm. in size at these altitudes and that these constitute approximately half the total debris population below 1500 Km. altitude.

This band of debris is termed "anomalous debris" in this paper because the debris density exceeded theoretical models by a large factor.

1.3. Scope of Paper

NASA/JSC funded an effort at Lincoln Laboratory to detect, track and characterize a sample set of debris in the anomalous debris band. While NASA's analysis used detection data of large numbers of debris in this band, we attempted to characterize in detail a small number of representative samples from this band using the radar and optical sensors operated by MIT Lincoln Laboratory. These sensors are located at Westford, MA, Kwajalein Atoll, Marshall Islands and White Sands Missile Range, New Mexico. The major purpose was to provide evidence supporting or contradicting the conclusions arrived at by NASA/JSC. In particular, our characterization involved the following steps:

1. Establish orbits on several debris from this band.
2. Determine the shape and size of the debris using radar data.
3. Assess the surface characteristics of the debris using visible wavelength optical data.
4. Compute the mass and density of the tracked debris.
5. Assess the state (solid/liquid) of the tracked debris.

The primary conclusion of this paper is that the properties of the debris sample tracked *are consistent with the hypothesis that they are Na-K coolant leak; and that they are likely to be in the liquid state.* The balance of this paper will describe the techniques used and individual results obtained to support this conclusion.

2. DEBRIS DETECTION

Three different strategies were used for the detection and acquisition of debris for characterization. These were:

1. Search orbits of putative parent satellites.
2. Stare and Chase using optical systems and radars.
3. Search the orbits of debris found

2.1. Orbit Search of Putative Parents

A quick assessment of the sensitivity of the Millstone radar (Fig. 3) and the putative size of the debris objects sought indicated that a new search mode needed to be created for the search. Historically the radar searches along the orbit. However, for the small objects considered here, it was

better to search at a relatively low range at an elevation of approximately 30 deg.; *ie.*, search along the orbit by staring at approximately the same range and the same elevation in the orbit of an object while letting time pass. Both the Haystack and the Millstone radars modified their software to construct this search mode.

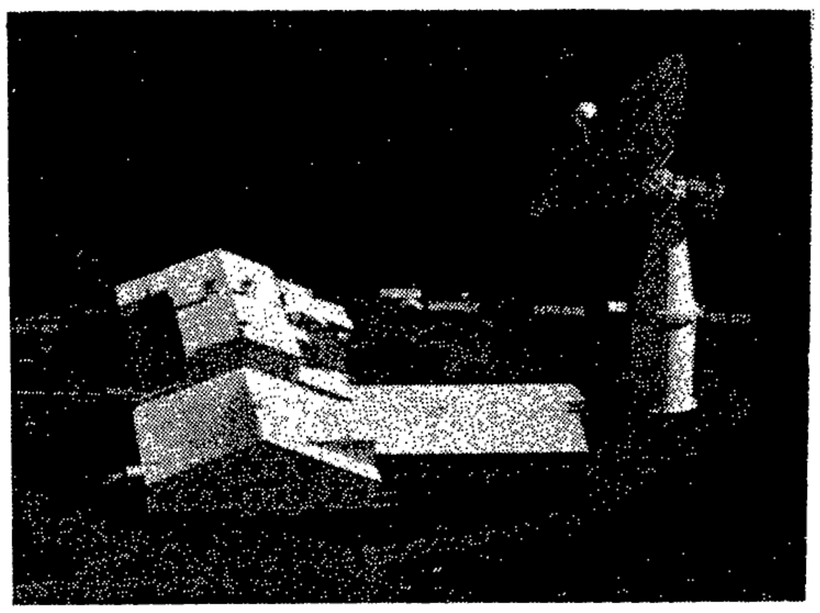

Fig. 3. Millstone Radar
(L-band, 1.3 GHz, 25 m. antenna, IFOV 8 mrad, S/N ratio of 50 dB on 1 sq. m. target at 1000 km.)

The Millstone radar searched the orbits of ten putative parents using this technique. The search was always centered about the parent to ensure that the parent was detected and thus validate the parameters of the search. The search mode was capable of detecting a 2 cm diameter object in orbit if coherently trackable[1] and approximately a 3.5 cm size object in orbit were it trackable non-coherently. No detections resulted.

If there were any recent slow leaks of debris of the size postulated, the difference in rate of change of the right ascension of the ascending node would have been small (<0.01 deg./day). *Hence it can be positively stated that none of the parent objects whose orbits were searched had recently (within 30 days of the search) leaked any debris of size >=2 cm.*

[1] The Millstone radar processes 2^N (N< 10) radar pulse returns together accounting for target movement during the integration interval. Were a target stable in attitude, the returns would add "coherently" yielding a combined S/N ratio of 2^N times that from a single pulse. If the target is tumbling, the returns would add "non-coherently" with a total S/N ratio of $2^{N/2}$ times that from a single pulse.

2.2. Stare and Chase - Optics and Radars

The Experimental Test System located in New Mexico (Fig. 4) is an optical system that was a proof of concept for the GEODSS. It has two 30 in. telescopes each with a FOV of $>1^0$ diagonal. The system uses a Vidicon camera and has a sensitivity of detection of ~15.5 V_M. The ETS conducted several stare-and-chase sessions for debris under Air Force sponsorship in 1994. The system is capable of detecting a resident space object, correlating it against the catalog and, if uncorrelated, transitioning from stare to tracking the object essentially in near-real-time (Ref. 5). ETS found one piece of anomalous debris that has been characterized extensively.

TRADEX is a L-band radar located on the Kwajalein atoll in the Marshall islands (Fig. 4). Its FOV is 0.5^0. TRADEX conducted several stare and chase sessions during 1995 under NASA/JSC sponsorship. The operating principle for TRADEX is the same as for ETS. The radar points at a specific azimuth and a specific high elevation and examines a range between 500 and 1200 Km. The radar's sensitivity is such that it should detect any object >3.5 cm in diameter in this altitude range. TRADEX detected one known and one uncorrelated RSO per hour on an average (Ref. 6). The radar found four pieces of anomalous debris during its operations.

2.3. Search of Anomalous Debris Orbit Planes

If the anomalous debris were a result of the leaking of a liquid, it seemed likely that there would be many "droplets" per orbit plane. Hence the orbit planes of some of the debris pieces found by ETS and TRADEX were extensively searched with the Millstone hill radar. The sensitivity of Millstone is such that it should detect any metallic sphere >2 cm in diameter in the search. Millstone found six more pieces of anomalous debris.

Finally, the Haystack radar searched some of the debris orbits. Haystack is the most sensitive of the radars used in this effort. It should detect debris of size >1 cm. Haystack found eight more debris objects though, unlike the eleven above, these were not completely characterized.

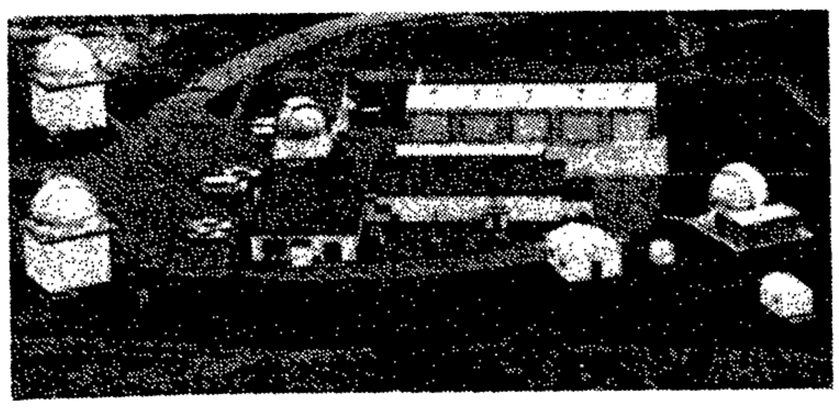

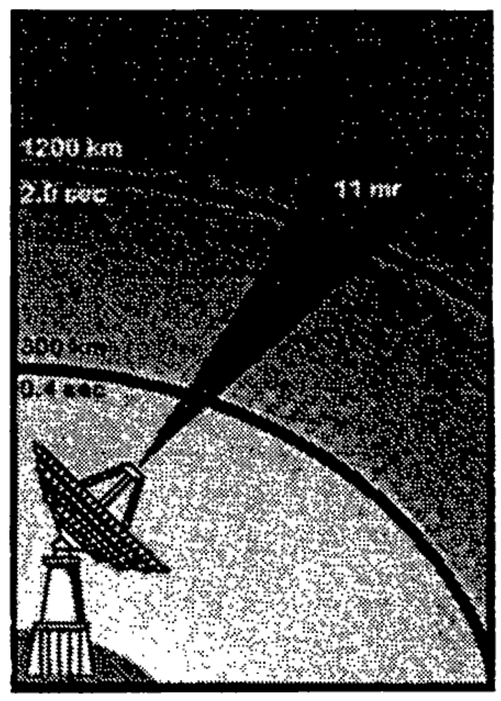

L-Band, 1320 MHz., IFOV 8 mrad,
48 dB S/N ratio on 1 sq.m. target at 1000 Km.

Fig. 4. ETS at White Sands Missile Range on left, TRADEX at Kwajalein on right.

2.4. Results of Searches for Anomalous Debris

The purpose of this project was to characterize a sample set of anomalous debris which required finding and tracking them regularly. A "time machine" search ws developed for the radars. The efficacy of the stare and chase algorithms at the radars was demonstrated. Eleven debris were found and extensively characterized. Eight more debris were found but were incompletely characterized.

A key finding is that there were multiple debris per orbit plane. This implies a common parentage and time of origin for these debris which is consistent with leaking liquid.

3. RADAR DATA ANALYSIS

Extensive data were collected with the Millstone and Haystack radars on the eleven debris found during the search. The objectives of the data collection were the following:

1. Radar signature data (radar cross-section vs. time) to assess spin period, any temporal variability and also to estimate size.
2. Polarization data (the ratio of the orthogonal polarization RCS to the principal polarization RCS) to assess the shape of the debris.
3. Metric data to support determination of accurate orbits and calculation of the area/mass ratios, mass and density of the debris.

Each of these topics will be discussed below.

3.1 Radar Signature and Polarization Data

Figure 5 is representative of the radar signature data on the debris as recorded at the Millstone radar. The radar transmits a right circularly polarized signal. The principal receive polarization (PP) is consequently left circular polarized; and the orthogonal receive polarization (OP) is right circular. The radar's tracking program dynamically selects the number of pulses integrated per signal processing cycle based on S/N ratio required for accurate metric tracking.

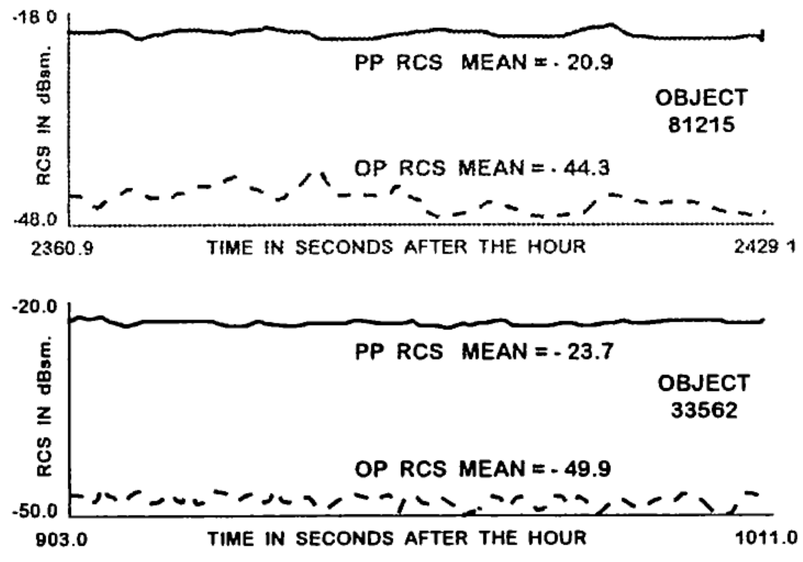

Fig. 5 : RCS signature in both polarizations of two debris

The figure shows the temporal history during a track (typically lasting 10 minutes) of the measured PP radar cross-section (RCS) for three of the debris. It is clear that the radar does not detect any temporal structure in the signal at a period longer than the integration interval which is 1 - 3 seconds. A number of tracks at a variety of aspect angles all exhibit invariant structure of the RCS at a temporal resolution of 1-3 seconds and

a RCS resolution of 1dBsm. The figure also shows the temporal history of the OP RCS during the same tracks. The OP RCS is below the PP RCS by ~ -25 dB. This is quite unusual based on over 300 tracks of typical debris that have been taken by the radar. Commonly, the OP / PP ratio is of the order of a few dB and varies over tracks (Ref. 7, also see Fig. 6).

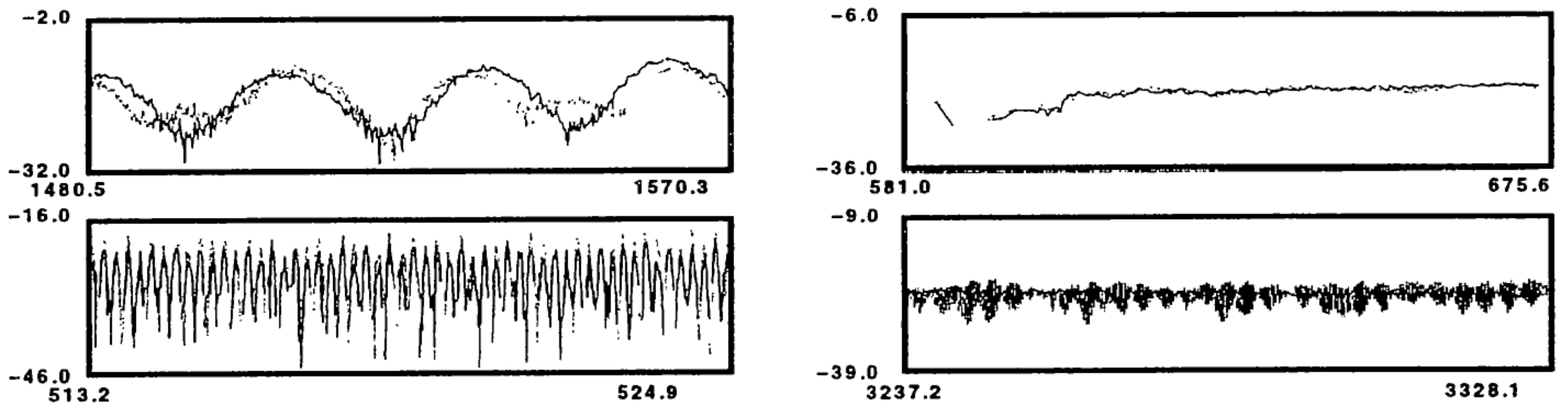

Fig. 6 : RCS signatures of typical debris at Millstone radar
[X- axis is time in secs. and Y-axis is RCS in dBsm
Solid line is PP RCS, Dotted line is OP RCS]

The accumulated statistics of mean PP RCS and the polarization ratio (OP RCS - PP RCS) for the eleven debris objects are given in Table 1. It is evident that, consistently, the PP RCS is < - 20 dBsm. and the polarization ratio is ~ -25 dB which is close to the isolation between the PP and OP channels at the Millstone hill radar.

It is well known that the OP return from spherical objects is negligible compared to the PP return *over all aspect angles for a circularly polarized radar transmission*. Comparison of the sphere RCS signature to those of the debris leads to the conclusion that the debris objects being tracked are spherical in shape. Further, the PP RCS of the debris can be used to infer a radius of the sphere. The results are shown in Table 1 along with the formal uncertainties based on a number of tracks.

TABLE 1 : Results from Millstone Data

OBJECT NUMBER	PP RCS MEAN (dBsm)	POLRZN RATIO (dB)	SPHERE MEAN RADIUS (cm.)	STD. DEV. (cm.)
81215	-20.8	-24.2	2.84	0.09
33562	-23.6	-21.6	2.55	0.06
33609	-22.4	-23.3	2.68	0.08
33612	-22.1	-25.3	2.71	0.05
33616	-30.7	-25.1	1.94	0.09
39969	-34.3	-21.2	1.70	0.08
39970	-32.3	-25.2	1.83	0.02
39971	-21.9	-24.5	2.73	0.03
39972	-22.1	-24	2.70	0.02
39973	-25.4	-21.2	2.38	
39974	-25	-25		

A few comments are in order here:

1. The range in radius of the spheres (1.6 cm. to 2.8 cm.) represents at the lower end the detection limit of the Millstone hill radar and at the upper end perhaps the largest size of the anomalous debris detected so far.
2. The estimated sphere size to radar wavelength ratio for the Millstone radar is well in the Rayleigh region. Hence there is no ambiguity in estimating the size from the RCS. Such an ambiguity would arise if the Haystack radar with its 3 cm wavelength were used for the purpose.
3. The formal uncertainties are based on the variability of the estimated mean radar cross-section in the principal polarization channel. No calibration corrections have been applied to these values. It is believed that the RCS estimate at the Millstone radar is good to <1 dBsm generally based on frequent tracks of a large 0 dBsm sphere. The same calibration uncertainty should apply to the small spheres in question because the radar attempts to track all objects at approximately the same S/N ratio (30 - 36 dB) and, further, this high S/N ratio is achievable in the case of the small spheres because of the high sensitivity of and the low slant range from the radar.
4. It is assumed that the spheres are perfectly conducting so that the radar theory relating the size to RCS as for example in Ref. 8 applies.

3.2. Density Estimation

It is well-known that the earth's atmosphere extends beyond the 800-1000 Km. orbital altitude of the anomalous debris. Hence, with accurate

metric data over many orbits, it is feasible to estimate an average area/mass ratio for the debris found in this project. Given that the debris are spherical, there is no dependence of the area/mass ratio on aspect angle. The area and volume can be calculated from the size reported in Table 1. Hence the mass and density can be computed.

The caveat in the chain of logic in the last paragraph is that the atmospheric density model at the altitudes of these anomalous debris is subject to considerable (~20%) uncertainty. This problem was solved by contemporaneous tracking of a well-characterized sphere - Lincoln calibration Sphere #4, SCC object no. 5398 - which happens to be in an orbit of similar altitude. Thus a scale factor for the atmospheric density could be estimated and used in fitting the metric data on the anomalous debris.

The metric data used came largely from the Millstone radar whose calibration is maintained extremely well. The quality of the data are shown in Table 2. The results of the procedure detailed above are shown in Table 3. It is evident that the "mean" density of the spheres is just over 1 gm/cc which is similar to that of water.

TABLE 2 : Millstone Hill Radar Data Accuracy

RCS DATA

BETTER THAN 1 dB.

METRIC DATA

RANGE : 5 METERS
ANGLES : 5 MDEG.
RANGE RATE : 10 mm/s

TABLE 3 : Mass and Density Estimates of Debris from Millstone Tracks

Object No.	Area-Mass Ratio (cm^2/gm)	Mass (grams)	Density (gms/cm^3)
81215	0.253+-0.007	100.2+-9.1	1.044+-0.06
33562	0.273+-0.066	74.8+-9.6	1.077+-0.11
33609	0.225+-0.011	100.2+-10.8	1.244+-0.10
33612	0.256+-0.006	90.1+-5.4	1.031+-0.04
33616	0.349+-0.009	33.8+-4.0	1.108+-0.08
39969	0.464+-0.22	19.6+-3.0	0.953+-0.09
39970	0.545+-0.043	19.3+-2.1	0.752+-0.07
39971	0.247	94.8	1.112
39972	0.307	74.6	0.905

"MEAN" DENSITY = 1.03 gms/cc

On the assumption that the anomalous debris are composed of Na-K, we looked up standard chemical tables for the density. The data on the Internet home page of Ref. 4 indicated that eutectic Na-K was probably used as the coolant in the nuclear power sources that were used on the Soviet satellites that are suspected to be the parents of these debris. Fig. 7 gives the variation of density of eutectic Na-K mixture with temperature drawn from Ref. 9. It is clear that the expected density of eutectic Na-K at ~300^0K is 0.9 gms/cc. similar to the density of the anomalous debris given in Table 3.

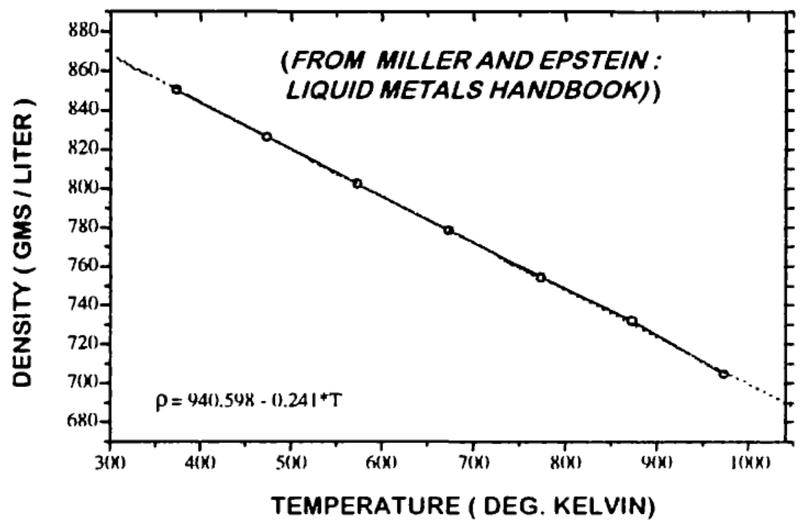

Fig. 7 : Density of Eutectic Na-K alloy vs. Temperature

3.3. Summary of Results from Radar Data Analysis

The following conclusions have been reached as a result of collection and analysis of signature, polarization and metric data from the radars.

1. The debris found and tracked exhibit without exception a polarization ratio at all aspect angles indicative of a spherical shape.
2. The debris found and tracked exhibit radii varying between 1.6 cm. and 2.8 cm.
3. The spheres have a mean density of ~1 gm./cc. consistent with eutectic Na-K at typical orbital temperatures.

4. OPTICAL DATA COLLECTION AND ANALYSIS

Earlier work (Refs. 10 - 13) has shown that some properties of the surface of debris reflecting sunlight can be derived from the analysis of photometric and polarimetric data. A photopolarimeter has been developed and fielded at the Firepond facility (Fig. 8) adjacent to the Millstone and Haystack radars.

All three sites are linked together with a real-time link such that any sensor can be driven off the pointing of any other sensor. This capability has been particularly valuable for Firepond as the photopolarimetric sensor has a narrow FOV.

Seven of the eleven debris objects have been characterized several times by the Firepond photopolarimeter. Examples of the photometric

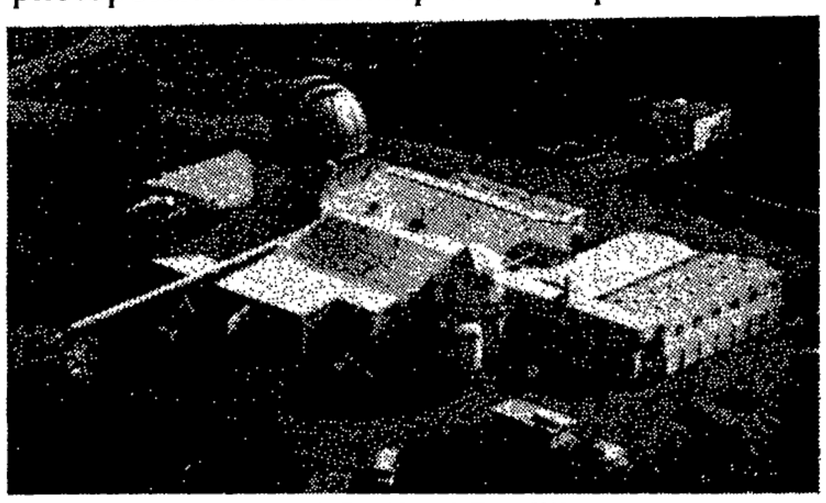

Fig. 8 : Firepond Optical Facility
1 meter optics with CCD photo-polarimeter
IFOV 1 mrad, ~ 13 m_v detection sensitivity

and polarimetric signature are shown in Figs. 9 and 10. For comparison, similar data on a sphere are also shown in Fig. 10. The following conclusions can be derived from these data:

dielectric surfaces. Hence all these objects appear to have metallic surfaces.

3. It is possible to assign (n,k) values that characterize the reflectivity of the surface. The calculated surface reflectance from (n,k) is high (>0.8) which is consistent with a specularly reflecting metallic surface.
4. Using the fact that these objects appear to be specular spheres, we can use the average brightness (estimated V_M at 1000 Km. Range) and the reflectivity to calculate the size of the objects.

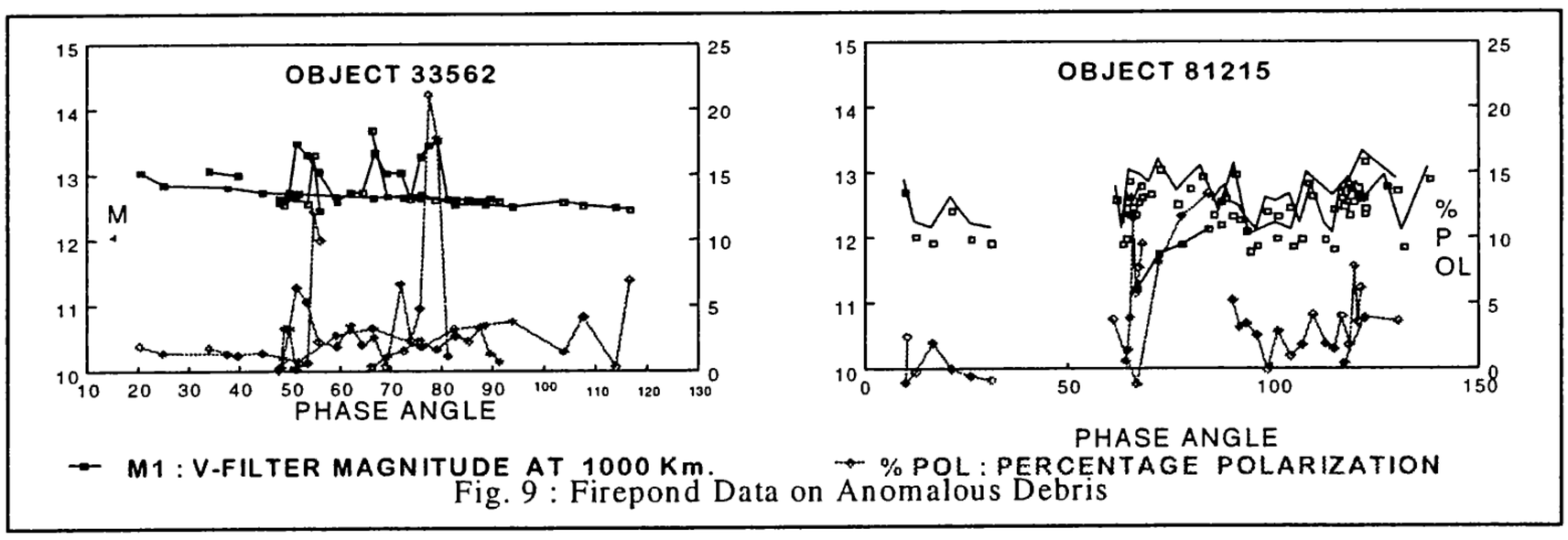

Fig. 9 : Firepond Data on Anomalous Debris

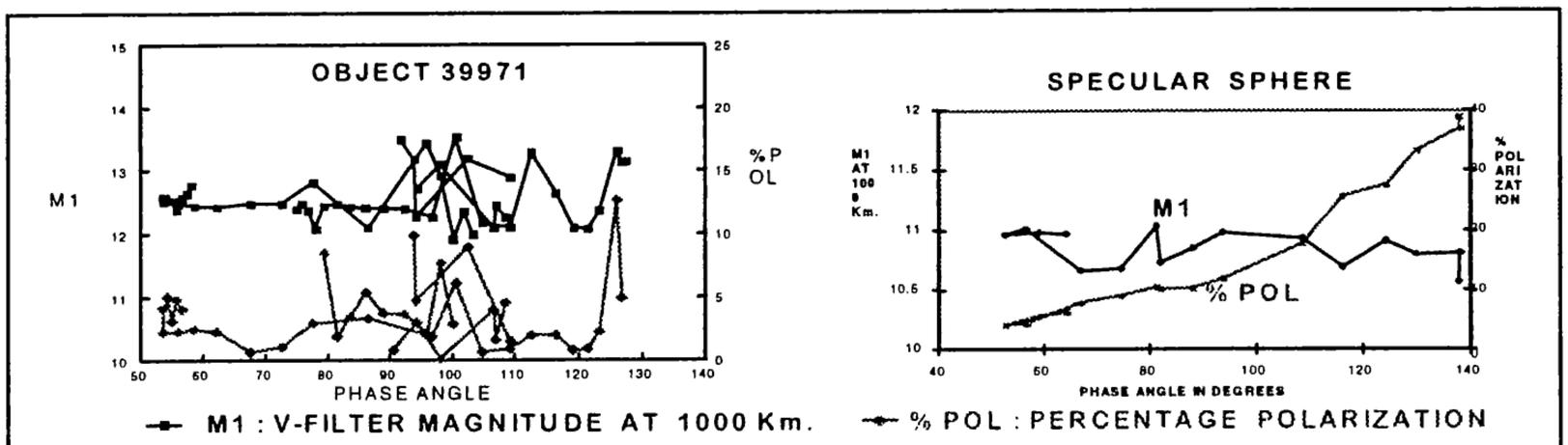

Fig. 10 : Firepond Data on Anomalous Debris and a Specular Sphere

1. The photometric phase functions (ie., derived V_M at a range of 1000 Km. vs. phase angle) on all seven objects are similar to that from specular spheres. This is highly unusual as typically debris tend to have a variety of shapes and phase functions.
2. The polarization is consistently low for all these objects. There is no evidence of high polarization that would be appropriate for

Table 4 gives the estimated M1 (V_M at 1000 Km. range) and the reflectivity of the seven objects characterized with optical data. Table 5 compares the estimated sizes of these from radar and optical data.

Table 4 : Measured M1 and Estimated Reflectance of Debris from Firepond Data

OBJECT	M1	R
33562	12.8+-0.3	0.89
33609	12.5+-0.2	0.84
39969	13.6+-0.08	0.89
39970	13.5+-0.2	0.89
39971	12.6+-0.4	0.89
39972	12.7+-0.3	0.89
81215	12.6+-0.4	0.88

Table 5 : Comparison of Estimated Sizes : Radar and Optical Data

OBJECT NUMBER	RADAR		OPTICAL	
	MEAN RADIU (cm.)	STD. DEV. (cm.)	MEAN RADIU (cm.)	STD. DEV. (cm.)
81215	2.84	0.09	2.9	0.5
33562	2.55	0.06	2.6	0.4
33609	2.68	0.08	3.0	0.3
33612	2.71	0.05		
33616	1.94	0.09		
39969	1.70	0.08	1.8	0.1
39970	1.83	0.02	1.8	0.1
39971	2.73	0.03	2.9	0.5
39972	2.70	0.02	2.9	0.4
39973	2.38			

There are some features of the plots that are not yet explained:

1. There is a small variation in the photometric phase function about a mean specular sphere characteristic that could be instrument-related, medium-related or surface property related. The first cause is unlikely because the instrument is calibrated to much better than the detectable variation. The second cause is unlikely as the variation is seen over many tracks. No explanation has been found as yet.
2. There have been occasional polarimetric data points showing substantially higher polarization than normal. The cause is unknown.

5. THEORETICAL ANALYSIS

The results presented in the previous sections strongly indicate that the anomalous debris are consistent with a Na-K fluid. Given the fact that the coolant was in a liquid state in the parent spacecraft, a question arises as to its state in orbit. We computed the expected temperature of the debris spheres using the known radiation from the sun and the earth, the properties of the orbit and of Na-K. We expect the maximum temperature in sunlight to be ~330^0 K and in shadow to be ~280^0K. The melting point of Na-K mixtures as a function of the mixture ratio is shown in Fig. 11. It is evident that the anomalous debris should in general be in a liquid state. This *may* affect the computation of the area-to-mass ratio as the drag coefficient C_d has been assumed to be 2.2 which applies to solids. It is not known at the present time whether atmospheric molecular scattering from liquids is similar to that from solids. This is an open area for further research. Further, we expect that liquid droplets will deform at some natural frequency but measurement has not been done to date.

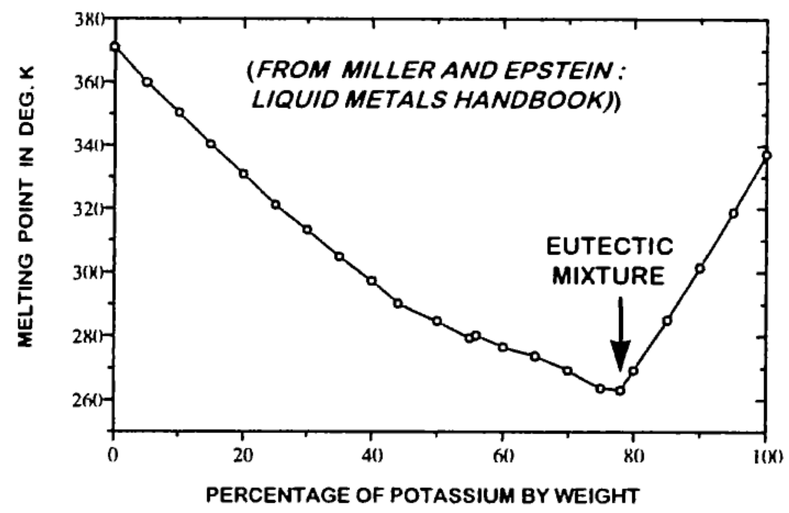

Fig. 11 : Melting Point of Na-K Mixtures

Another question is the lifetime of liquid Na-K droplets in orbit due to evaporation. This has been modeled using data available in Chemistry handbooks (Ref. 10) and our calculation show that the lifetime for a 2.5 cm. diameter sphere is > 10000 years if the debris were made of either pure Na or pure K.

A third question is the orbital lifetime of the Na-K spheres due to atmospheric drag. In particular, are these debris likely to pose a hazard to humans in space at 300-500 Km. altitudes? Given the calculated area-to-mass ratios of the detected spheres and extrapolating to 1 mm. radius debris, the orbital lifetime is well over 50 years.

6. SUMMARY

The project has demonstrated a powerful capability for remote sensing and characterization of orbital debris using ground-based radar and optical systems. A small sample from a particularly profuse debris field has been characterized with the following results:

1. The nature of the debris is consistent with leaked Na-K fluid but remote sensing done to date cannot prove this unambiguously.

2. The debris cluster in several orbit planes with many pieces of various sizes in each plane. Both of these features are consistent with a leaking liquid from a set of parents from the RORSAT set of Soviet satellite systems.
3. No recent leak has been detected. Further the last such satellite was launched in 1989. These facts would seem to indicate that the leaks occurred soon after the nuclear power sources were put into their rest orbits as inferred by NASA/JSC.
4. All the debris detected and tracked were spherical in shape with radii < 2.8 cm. The sphericity is again consistent with a leaking liquid.
5. The estimated density of the sample set is ~1 gm/cc which is consistent with Na-K mixture.
6. The debris are highly reflective and exhibit characteristics of specular metallic spheres - again consistent with droplets of Na-K.
7. If the debris are indeed Na-K and if, as indicated by the Russian manufacturers, it is an eutectic mixture, then the droplets are expected to be in liquid form due to heating by the sun and the earth.
8. If the debris are droplets of Na or K, the rate of evaporation is so low that their lifetimes exceed 10000 years.
9. The combination of orbital altitude and area/mass ratio is such that the orbital lifetime due to atmospheric drag is expected to exceed 50 years for even a 1 mm. size particle.

To reiterate, analysis of all the measurements done to date on the sample debris are consistent with leaking liquid Na-K but do not unambiguously prove the assertion.

7. REFERENCES

1. E.G.Sansbery *et al* : "Haystack Radar Measurements of the Orbital Debris Environment", JSC-26655, NASA/JSC Space & Life Sciences Directorate, May 20, 1994.
2. E.G.Sansbery *et al* : "Haystack Radar Measurements of the Orbital Debris Environment: 1990-1994" , JSC-27436, NASA/JSC Space & Life Sciences Directorate, 20 April 1996.
3. E.G.Stansbery *et al*: "Orbital Debris Studies Using the Haystack Radar", presented at the 1995 Space Surveillance Workshop, 29 March 1995.
4. Internet address, Russian RORSAT contacts, http://www.rssi.ru/ippe/general/spacer.html.
5. Private communication.
6. Ray LeClair, et al: "Improvements in TRADEX Debris Capabilities", presented at the 1996 Space Surveillance Workshop, 3 April 1996.
7. R. Sridharan, "Characteristics of Debris and Implications for Detection and Tracking", AAS 96-117, presented at the AAS/AIAA Space Flight Mechanics Meeting, Austin, Texas, 12-15 February 1997.
8. Radar Cross-Section Handbook, Editor: George T. Ruck, Plenum Press, New York – London, 1970.
9. R.R. Miller in, Liquid Metals Handbook, Sodium (NaK) Supplement, C.B. Jackson (ed.), Atomic Energy Commission and the Dept. of the Navy, 1955.
10. Smithsonian Physical Tables, W.E. Forsythe (ed.), Smithsonian Institution, Washington, DC, 1964.
11. Private communication.
12. Private communication.
13. Private communication.